2012

Experimental Investigation on a Reversible Heat Pump for a Passenger Car

Vincent Lemort
vincent.lemort@ulg.ac.be

Cristian Cuevas

Sébastien Declaye

Experimental Investigation on a Reversible Heat Pump for a Passenger Car

Vincent LEMORT[1]*, Cristian CUEVAS[2], Sébastien DECLAYE[1]

[1]Thermodynamics Laboratory, University of Liège, Belgium
Vincent.Lemort@ulg.ac.be

[2] Facultad de Ingeniería Mecánica, Universidad de Concepción, Chile
crcuevas@udec.cl
* Corresponding Author

ABSTRACT

This paper summarizes the first results of a research project dealing with the development of a reversible heat pump for a passenger car. Heat pump systems appear to be a more efficient alternative to electrical resistance heaters for the purpose of heating the car indoor environment. Heat pump systems could be easily implemented into cars by allowing the air-conditioning system to run in reverse. In order to check the technical feasibility of a reversible heat pump system, and to point out technical barriers, a prototype was built and tested. Experimental data was also used to calibrate and validate simulation models of components. A heat pump system model was finally built to investigate the operating conditions of the system.
The first part of the paper describes the test rig (architecture, components, and measurement devices) and the experimental campaign. Performance of components (compressor, evaporator, condenser and heater core) is evaluated in terms of variation with the operating conditions.
The second part of the paper presents the steady-state semi-empirical models of the components. Such lumped models retain and concentrate the main physical phenomena inherent to the components into successive elementary processes (pressure losses, heat transfers, etc.). They require a limited number of parameters that can be identified based on experimental data. The calibration and the validation of the proposed component models are detailed. Finally, an overall simulation model of the reversible heat pump system is proposed and used to evaluate the energy performance of the system as function of the operating conditions.

1. INTRODUCTION

Electrical Vehicles (and Hybrid Electrical Vehicles) do not beneficiate from the heat released into the engine cooling system to heat the cabin. One solution consists in using electrical resistance heaters, which would cut-off significantly the driving range of the vehicle. A more efficient option would consist in using a vapor compression heat pump in conjunction with back-up electrical resistances.

This paper aims at investigating the energy performance of a retrofitted mobile air-conditioning system working as a reversible heat pump. The proposed system is represented in Figure 1. It comprises the following main components: a parallel multi-flow heat exchanger (placed in front of the vehicle and working as an evaporator in heating mode and as a condenser in cooling mode), a variable displacement wobble plate compressor, and an air-conditioning module (comprising the AC evaporator, the heater core and a centrifugal fan). Refrigerant is R134a. With respect to the original mobile air conditioning system, 3 additional components are introduced: a four-way valve (to reverse the cycle), a water-cooled condenser and a two-way valve (to by-pass the water-cooled condenser).

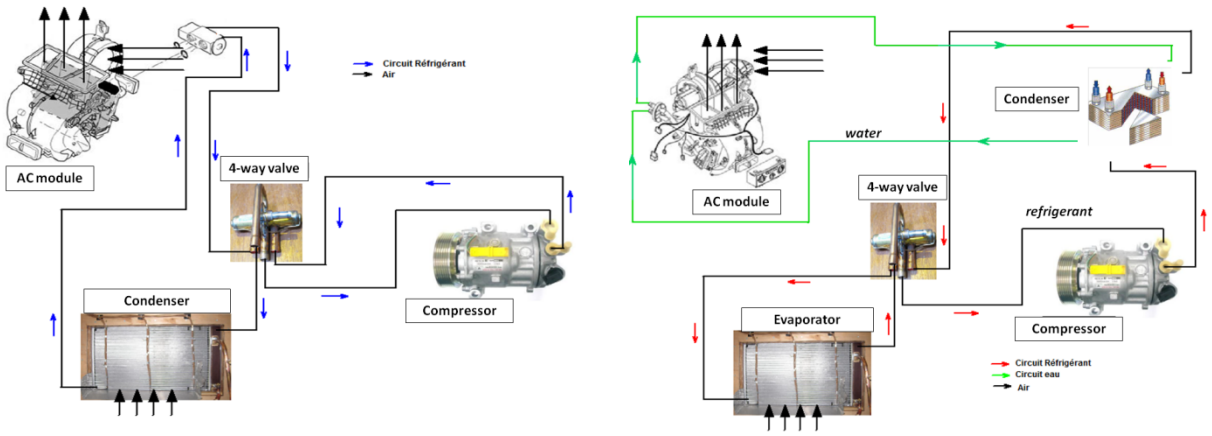

Figure 1: Retrofitted reversible heat pump system (left: cooling mode / right: heating mode)

The system works as an air-to-air refrigerator but as an air-to-water heat pump. The latter type of heat pump has been preferred to an air-to-air heat pump (already investigated by Pommé (1997)) in order to modify as little as possible the original configuration of the vapor compression system and of the air-conditioning module. With such a configuration, the water-cooled condenser is placed in series with the internal combustion engine on the hot (glycol) water loop feeding the heater core (inside the AC module).

2. EXPERIMENTAL INVESTIGATION

2.1 Description of the Test Rig

In order to evaluate the energy performance of the reversible heat pump system, the latter was coupled to two air loops: one controlling the air feeding the front heat exchanger ("outside air loop") and one controlling the air entering the air-conditioning module ("cabin air loop"). Attention was paid to set-up a refrigerant circuit as representative as possible to the one integrated inside the vehicle. More specifically, pipe lengths and bends were selected in such a way not to introduce to many pressure losses in comparison with the real application. As shown in Figure 2, the major modification done on the refrigerant circuit consisted in introducing a Coriolis flow meter in order to measure accurately the refrigerant flow rate. This flow meter is surrounded by different two-way valves in order to ensure that the refrigerant always flows in the same direction whatever the operating mode of the system.

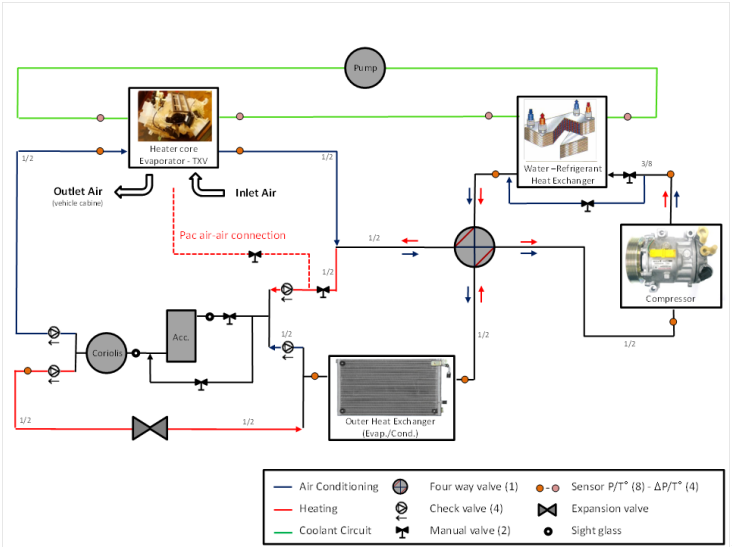

Figure 2: Schematic representation of the instrumented refrigerant circuit

Pressures and temperatures (thermocouples) are measured at the inlet and outlet of the major components of the circuit. The air loop, in which the front heat exchanger is integrated, allows for the control of the air speed as well as the air temperature and relative humidity at the inlet of the heat exchanger. As shown in Figure 3, the air loop is equipped with a set of nozzles in order to measure the air flow rate. Temperature and relative humidity are measured in several locations in the inlet and outlet of the heat exchanger.

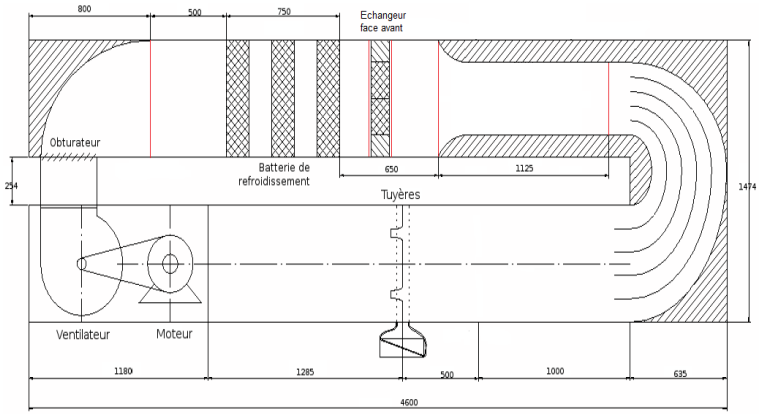

Figure 3: Air loop simulating the outside air conditions in front of the vehicle

In order to decrease the air temperature at the inlet of the heat exchanger down to -15°C, the air loop can be fed by cold air prepared by an air-cooler. Also the latter can be supplied by dry air coming from an air drier in such a way to measure the performance of the heat pump in the absence of frosting.
The air flow feeding the AC module results from the mixing between ambient air and air coming from the air-cooler.
The compressor is placed inside a calorimeter in order to evaluate the heat transfer to the ambient. The air temperature inside the calorimeter is controlled by means of a water cooling coil and light bulbs. The compressor shaft power is deduced from the simultaneous measurements of the shaft torque and rotational speed. The later is adjusted by means of an inverter.

2.2 Testing campaign

In total, 84 points in steady-state regime were achieved: 51 points in heating mode (dry conditions, i.e. without any frost in the evaporator) and 33 points in cooling mode. The investigated variables were the outside air temperature, the air flow rate in the AC module, the air flow rate through the front heat exchanger, the glycol water flow rate and the rotational speed of the compressor.

2.3 Performance Analysis

This section focuses on the performance analysis in heating mode. The evolution of the performance of the compressor with its rotational speed and the ratio between the discharge and the suction pressures is shown in Figure 4. It can be observed that, at reasonable rotational speeds, large pressure ratios are imposed to the machine. This is explained by several elements: the temperature lift between the heat source and heat sink is larger in heat pump mode than in refrigerator mode, an additional temperature pinch is introduced in the system because of the presence of an intermediate hot water loop between the refrigerant and the cabin air, and the pressure losses through the front heat exchanger are much larger in evaporator than condenser modes (see Figure 6). The decrease of the compressor performance with the rotational speed is partially due to the increase of the suction pressure losses and the re-expansion of the clearance volume (which decreases the volumetric performance of the machine as indicated in Figure 4 b)). The evolution of the measured COP as function of the pressure ratio imposed to the compressor is given in Figure 5.

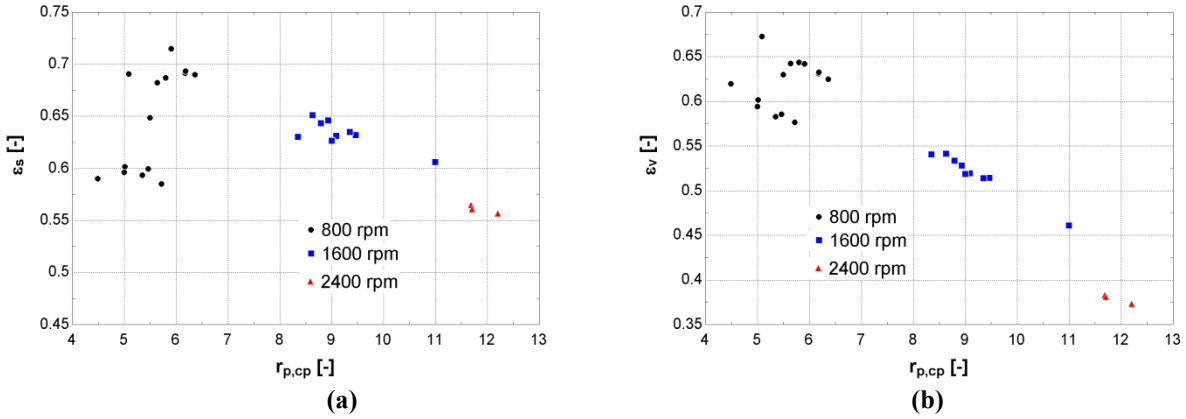

Figure 4: Evolution of the performance of the compressor with the pressure ratio and the rotational speed ((a): isentropic effectiveness; (b): volumetric effectiveness)

Figure 6 shows the evolution of the pressure losses through the front heat exchanger, in cooling and heating modes, with a parameter that is a constant multiple of the dynamic pressure at the heat exchanger inlet. It can be observed that pressure losses are much more important in heating mode than in cooling mode.

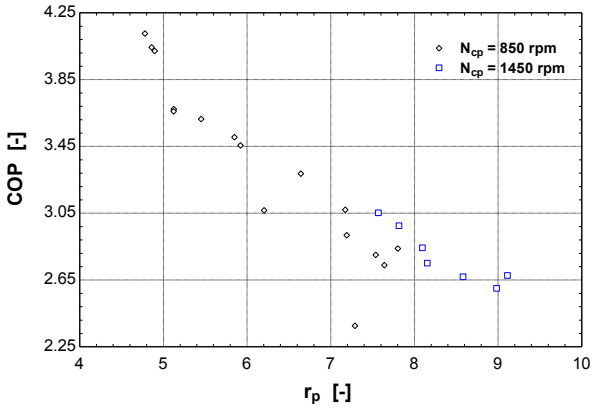

Figure 5: Measured COP vs compressor pressure ratio

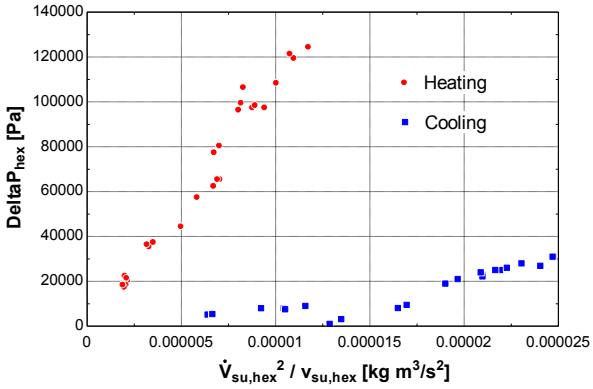

Figure 6: Pressure losses through the front heat exchanger

It was difficult to vary the parameters of the system independently. Hence, the sensitivity of the system performance with the operating conditions is analyzed by comparing pairs of points for which only one parameter has been varied. Comparison of points 3 and 4 stresses the strong influence of the compressor rotational speed. The decrease of the COP with the rotational speed is due to the increase of the pressure ratio and compressor mechanical losses. Increasing the cabin supply air flow rate allows decreasing the condensing pressure and hence the pressure ratio (comparison of points 5 and 6).

Table 1: Performance of the reversible heat pump in heating mode as function of the outside temperature, compressor rotational speed and cabin supply air flow rate

	Outside temperature (°C)	Heating capacity (kW)	COP	Cabin supply temperature (°C)	Pressure ratio
1	-11.3	1.92	3.83	17.3	5.01
2	0.9	2.78	3.82	30	5.09

	Rotational speed (rpm)	Heating capacity (kW)	COP	supply temperature	Pressure ratio
3	1606	3.5	2.69	36.1	8.35
4	805	2.78	3.82	30	5.09

	Cabin supply air flow rate (kg/s)	Heating capacity (kW)	COP	Cabin supply temperature (°C)	Pressure ratio
5	0.136	1.96	4.07	12.6	4.49
6	0.085	1.87	3.59	20.8	5.47

2. MODELING AND SIMULATION

2.1 Modeling of the components

A steady-state simulation model of the heat pump was developed by associating the models of the different components of the system. For the wobble plate compressor, the simulation model proposed by Cuevas et al. (2008) was considered. This lumped simulation model accounts for the major losses: supply pressures losses, expansion of the clearance volume, heat transfers and mechanical losses. Parameters of the model were identified by minimizing a function accounting for the errors on the prediction of the consumed shaft power, displaced mass flow rate and discharge temperature. These parameters are given in Table 2.

Table 2: Identified parameters of the wobble plate compressor, evaporator, condenser and heater core models

V_s	145.8 cm³
α	0.2657
$\dot{W}_{loss0}$	56.5 W
δ_{su}	0.124
c_f	0.0366
AU_{amb}	7.486 W/K
AU_{su_n}	400 W/K
AU_{ex_n}	6.161 W/K

K_1	0,2889
K_2	0,9933
K_3	1,183
K_4	$5{,}478\ 10^9$
K_5	0.204
K_6	1.35
K_7	$1.665\ 10^9$

C_a	752.7
C_w	15000

As shown in Figure 7, the compressor simulation model is able to predict the performance of the machine with a good accuracy.

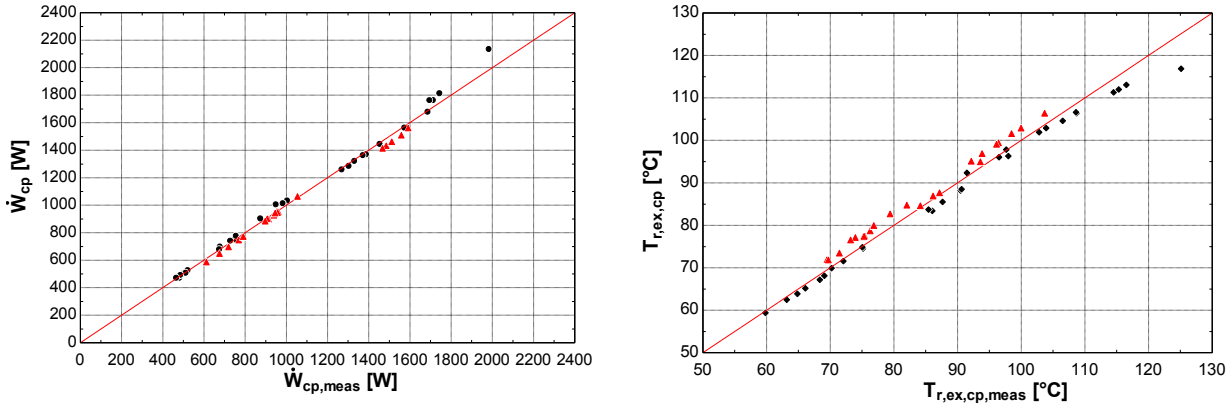

Figure 7: Simulation model of the compressor: predicted vs measured values (left: shaft power; right: discharge temperature)

The front heat exchanger was modeled as a cross-flow heat exchanger with 2 zones on the refrigerant side. In the single phase zone, either the correlation of Dittus Boelter or the correlation of Shah is used according to the regime of the refrigerant flow inside the tubes. Shah's correlation has been corrected by a factor K_1.

$$h_{lam} = K_1\, 0.488\, (f\,Re)^{1/3} \left(\frac{L}{D_h\, Re\, Pr}\right)^{-1/3} \left(\frac{k}{D_h}\right) \tag{1}$$

$$h_{turb} = 0.023\, Re^{0,8}\, Pr^{n} \left(\frac{k}{D_h}\right) \tag{2}$$

In the two-phase zone, the heat transfer coefficient was estimated by means of the correlation of Wattelet *et al.* (1994) corrected by a coefficient K_2.

$$h = K_2\left[h_{nb}^{2,5} + h_{cb}^{2,5}\right]^{1/2,5} \tag{3}$$

The convective coefficient on the air side is given by the correlation of Chang and Wang (1997), also corrected by a coefficient K_3.

$$h = K_3 Pr^{1/3}\, Re_{Lp}^{0,51} \left(\frac{\theta}{90}\right)^{0,27} \left(\frac{F_P}{L_p}\right)^{-0,14} \left(\frac{F_h}{L_p}\right)^{-0,29} \left(\frac{T_d}{L_p}\right)^{-0,23} \left(\frac{L_l}{L_p}\right)^{0,68} \left(\frac{T_p}{L_p}\right)^{-0,28} \left(\frac{F_t}{L_p}\right)^{-0,05} \left(\frac{k}{D_h}\right) \tag{4}$$

The pressure loss on the refrigerant side in the two-phase zone is estimated by the following correlation whose parameter K_4 must be identified.

$$\Delta P_{tp} = K_4\, \frac{\dot{M}_r^{\,2}}{\rho_{r;tp}} \tag{5}$$

Parameters of the model were identified in order to best predict the inlet and outlet pressures of the evaporator. The quality of the calibrated model is evaluated in Figure 8. The accuracy of the model is judged acceptable.

The water cooled condenser is modeled as a counter flow heat exchanger with 3 zones on the refrigerant side. The heat transfer coefficients in the liquid and vapor zones are estimated by means of Martin correlation corrected by a factor K_5. The heat transfer coefficient in the two-phase zone is estimated by the correlation of Yan *et al.*, described in the work of Garcia-Cascales et al. (2007), corrected by a factor K_6. Pressure drop in two-phase zone is computed by means of Equation (5) whose coefficient is K_7.

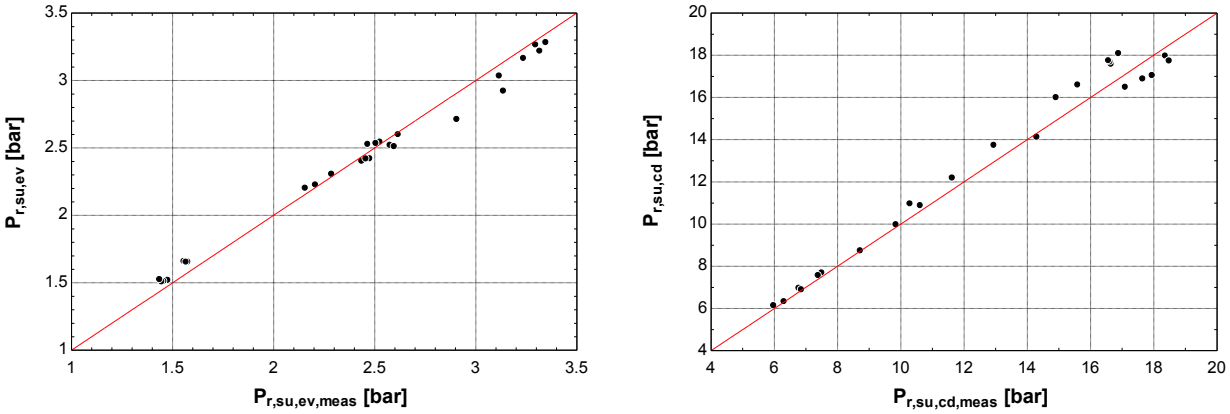

Figure 8: Simulation model of the heat pump evaporator (a) and condenser (b): predicted vs measured values of the supply pressures

The heater core was modeled by using the epsilon-NTU method. The overall heat transfer coefficient of the heat exchanger was computed by associating two lumped heat transfer resistances in series: one on the water-side and the other on the air-side. These resistances are assumed to vary with the air and water flow rates according to Equation (7) whose coefficients are given in Table 2.

$$AU_{heater} = (R_a^* + R_w^*)^{-1} \tag{6}$$

$$\frac{1}{R_a^*} = C_a \dot{M}_a^{0.6} \qquad \frac{1}{R_w^*} = C_w \dot{M}_w^{0.8} \tag{7}$$

The validity of the heater core model is shown in Figure 9, which compares the predicted and the measured heat exchanger outlet air and water temperatures.

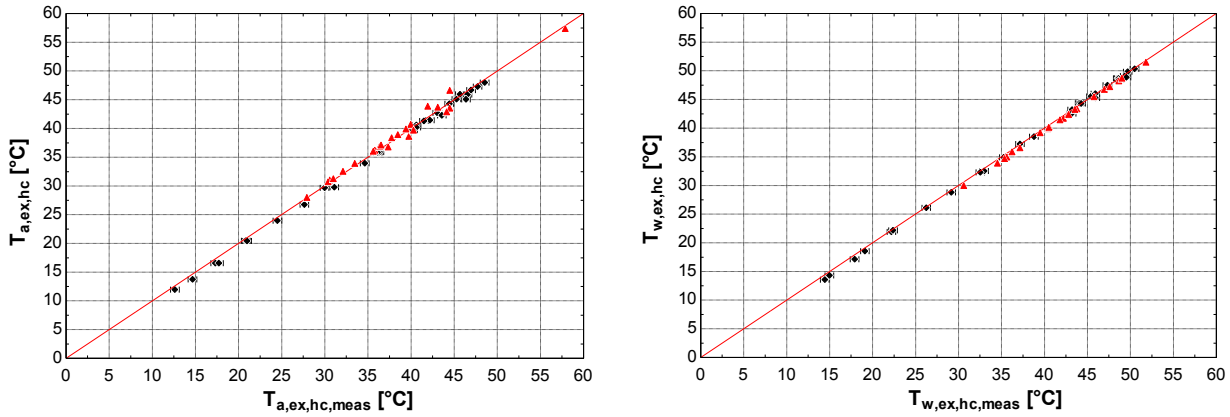

Figure 9: Simulation model of the heater core: predicted vs measured values of the air (a) and water (b) outlet temperatures

2.1 Simulation of the heat pump system

The investigated air-to-water heat pump is modeled in order to evaluate the influence of the operating conditions on the performance of the system. The heat pump model is built by associating the models of each components presented hereunder. The heat pump model is coupled to a simple thermal model of a cabin in order to account for the variation of the heating load with the outside air temperature. The evaporator model does not account for frost formation and hence frosting-defrosting cycles are not described.

First, the influence of the rotational speed is investigated. The latter is varied between 500 and 5000 rpm for 4 outside air temperatures (-8°C, -5°C, 0°C and 5°C). The recirculation rate is set to 40%. The air mass flow rate supplied to the cabin in adjusted in order to achieve a pulsion temperature of 45°C. It can be observed in Figure 10 that the isentropic effectiveness and the COP of the system are sharply decreasing with the rotational speed of the compressor. This is due to the increasing compressor supply pressure losses, mechanical losses and losses associated to the clearance volume. Figure 11 shows that, at a compressor rotational speed of 5000 rpm, a cabin temperature of 22°C (corresponding to the comfort) cannot be reached for outside air temperatures lower than -6°C.

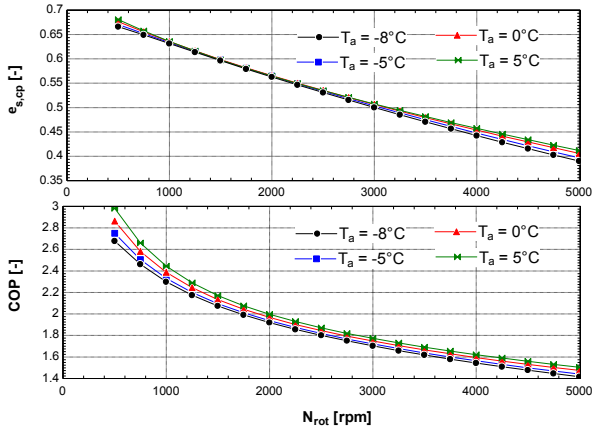

Figure 10: Compressor isentropic effectiveness and heat pump COP vs rotational speed

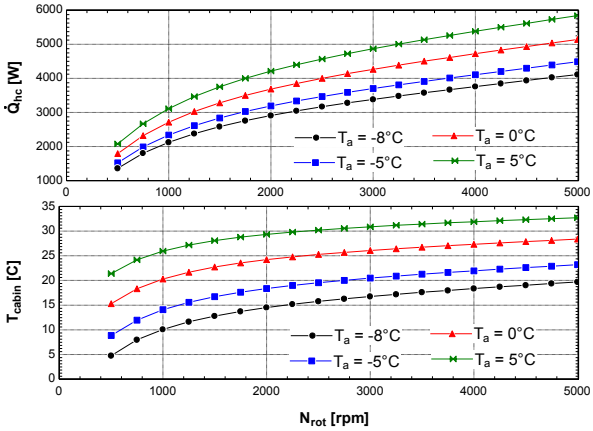

Figure 11: Heater core thermal power and cabin temperature vs rotational speed

Previous results indicate that the heat pump alone would not be able to ensure the required comfort in the cabin for low outside air temperatures. Moreover the heat pump COP is very sensitive to the compressor rotational speed and thus to the heat pump capacity. The following simulation, carried out considering a maximal compressor displacement, aims at investigating to what extent an electrical resistance heater should be used in conjunction with the heat pump (in series with the heater core) to ensure the thermal comfort. For each point of the simulation, the power of the electrical resistances is adjusted in order to maximize the global COP of the system. The latter accounts for the electrical consumption of the resistances and the equivalent electrical consumption of the compressor (assuming an electrical motor efficiency of 90%). The rotational speed of the compressor and the power of the resistances leading to a cabin temperature of 22°C are computed. The air flow rate is varied to achieve a supply temperature of 45°C. Figure 12 gives the evolution of the heater core thermal power, compressor consumption and resistances power as function of the outside air temperature. Simulation indicates that underneath 0°C, it is preferable not to operate the compressor at its maximal rotational speed and to provide part of the required heating load by means of resistances. This allows decreasing the condensing pressure and, combined with the decrease of the compressor rotational speed, increasing the compressor isentropic effectiveness and the COP of the heat pump.

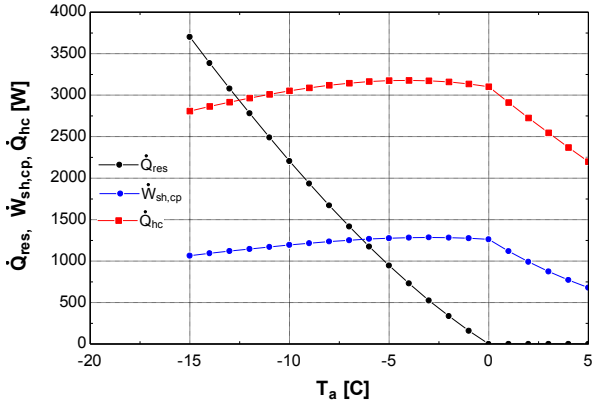

Figure 12: Electrical, mechanical and thermal powers vs outside air temperature

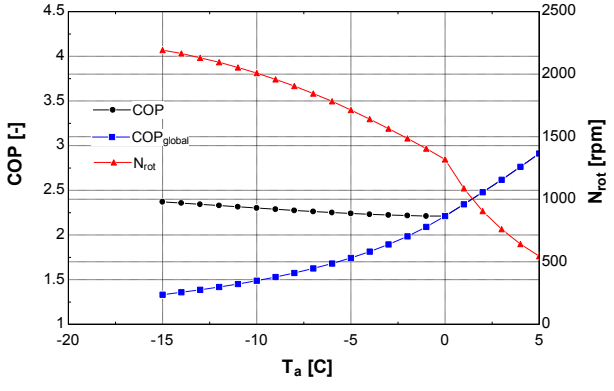

Figure 13: COP and rotational speed vs outside air temperature

As shown in Figure 13, the optimal speed of the compressor is maintained underneath 2500 rpm, which allows maintaining good isentropic effectiveness of the compressor. The COP of the heat pump remains close to 2.3 and the global COP is decreasing due to use of the electrical resistances.

3. CONCLUSIONS

The proposed retrofitted heat pump system is rather simple, with only few additional components in comparison with the original mobile air conditioning system.
The experimental study carried out on the prototype of heat pump system indicated that large pressure ratios are imposed to the compressor (larger than in cooling mode), which has a strong impact on the compressor performance. The design of the front heat exchanger is not well adapted to the heat pump mode. Pressure losses represent up to 40% of the supply pressure, while it is only 2% in cooling mode.
A simulation model of the whole heat pump system was built by associating calibrated and validated models of its different components. Simulation of the whole system indicated that for temperatures lower than -6°C electrical resistances must be used in order to ensure the thermal comfort in the cabin (considering a comfort temperature of 22°C, a supply air temperature of 45°C, a recirculation rate of 40% and a rotational speed of the compressor of 5000 rpm). Moreover, when the compressor displacement is set to its maximum value, the power provided by the electrical resistance heater could be adjusted in such a way to maximize the energy performance of the global heating system (heat pump + resistances).

ADDENDUM

Another simulation is carried out where the speed of the compressor is imposed and the displacement of the compressor is adjusted in order to maintain a cabin temperature of 22°C. Electrical resistances are used when the maximal compressor displacement is reached. Figure 14 indicates the evolution of the heat pump overall COP with the outside air temperature for different rotational speeds. A COP close to 1.5 is achieved for an outside air temperature of -10°C.

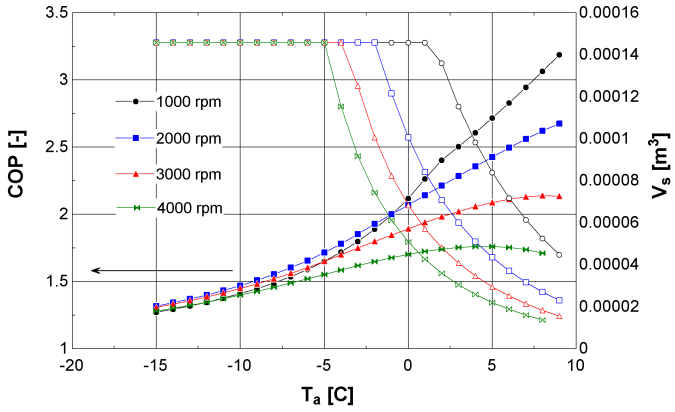

Figure 14: Overall COP and compressor displacement vs outside air temperature

NOMENCLATURE

α	proportional losses	(-)	**Subscripts**
α	fraction of area	(-)	a air
AU	heat transfer coefficient	(W/K)	amb ambient

C	coefficient	(-)	cb	convective boil.
c_f	clearance volume factor	(-)	cd	condenser
D	diameter	(m)	cp	compressor
δ	dimensionless diameter	(-)	ev	evaporator
ΔP	pressure loss	(Pa)	ex	exhaust
F_d	fin depth	(m)	h	hydraulic
F_h	fin height	(m)	hc	heater core
F_p	fin pitch	(m)	lam	laminar
F_t	fin thickness	(m)	meas	measured
h	convective heat transfer coeff.	(W/m^2-K)	n	nominal
k	thermal conductivity	(W/m-K)	nb	nucleate boiling
K	coefficient	(-)	res	resistances
L_h	louver height	(m)	su	supply
L_l	louver length	(m)	tp	two-phase
L_p	louver pitch	(m)	turb	turbulent
Θ	louver angle	(°)	w	water
T_t	tube length	(m)		
T_d	tube depth	(m)		
T_p	tube pitch	(m)		
T_h	tube major diameter	(m)		
V_s	compressor displacement	(cm^3)		
$\dot{W}_{loss0}$	constant losses	(W)		

REFERENCES

Cuevas, C., Winandy, E., Lebrun, J., 2008, Testing and modeling of an automotive wobble plate compressor, *Int. J. Refrig*., vol. 31: p. 423-431.

Chang Y. and Wang C. 1997. A generalized heat transfer correlation for louver fin geometry. *Int. J. of Heat and Mass Transfer*, Vol. 40, No. 3, p. 533-544.

Garcia-Cascales J.R., Vera-Garcia F., Corberan-Salvador J.M. et Gonzalvez-Macia J. 2007. Assessment of boiling and condensation heat transfer correlations in the modeling of plate heat exchangers. *International Journal of Heat and Mass Transfer*, Vol. 30, pp. 1029 - 1041.

Pommé, V., 1997, Reversible Heat Pump System for an Electrical Vehicle, *SAE Technical Paper* 971772.

Wattelet J., Chato J., Souza A. and Christoffersen B. 1994. Evaporative characteristics of R12, R134a, and a mixture at low mass fluxes. ASHRAE Transactions, Vol. 100, Part 1, pp. 603-615.

ACKNOWLEDGEMENT

The authors would like to thank Mr. Renaud Delfosse who carried out part of the measurements.